Measurements of quantum noise in resistively shunted Josephson junctions

Roger H. Koch, D. J. Van Harlingen,* and John Clarke
Department of Physics, University of California, Berkeley, California 94720
and Materials and Molecular Research Division, Lawrence Berkeley Laboratory,
Berkeley, California 94720
(Received 19 November 1981)

Measurements have been made of the low-frequency spectral density of the voltage noise in current-biased resistively shunted Josephson tunnel junctions under conditions in which the noise mixed-down from frequencies near the Josephson frequency (ν_J) to the measurement frequency ($\ll\nu_J$) is in the regime $h\nu_J > k_BT$. In this limit, quantum corrections to the mixed-down noise are important. The spectral densities measured on junctions with current-voltage characteristics close to the Stewart-McCumber model were in excellent agreement with the predicted values, with no fitted parameters. The mixed-down noise for a wide range of bias voltages was used to infer the spectral density of the current noise in the shunt resistor at frequency ν. With no fitted parameters, this spectral density at frequencies up to 500 GHz was in excellent agreement with the prediction $(2h\nu/R)\coth(h\nu/2k_BT)$. The presence of the zero-point term, $2h\nu/R$, at frequencies $h\nu > k_BT$ was clearly demonstrated. The current-voltage characteristics of a junction with $\beta_L \equiv 2\pi L_s I_0/\Phi_0 \sim 1$ and $\beta_C \equiv 2\pi I_0 R^2 C/\Phi_0 \ll 1$, where I_0 is the critical current, C is the junction capacitance, and L_s is the shunt inductance, showed structure at voltages where the Josephson frequency was near a subharmonic of the L_sC resonant frequency. The additional nonlinearity of the I-V characteristic caused mixing down of noise near higher harmonics of the Josephson frequency, thereby greatly enhancing the voltage noise. The measured noise was in good agreement with that predicted by computer simulations.

I. INTRODUCTION

The effects of thermal noise on a resistively shunted[1,2] Josephson[3] junction (RSJ) have been extensively studied. The theories assume that the noise originates as Nyquist noise in the shunt resistor R. The junction is modeled as a particle moving in a tilted periodic potential, and the effect of the noise current is to induce random fluctuations in the angle of tilt. These fluctuations have two effects. First, they enable the phase of the junction to slip by 2π when the bias current I is less than the noise-free critical current I_0, thereby producing a voltage pulse across the junction. This effect produces noise rounding of the I-V characteristics at low voltages, V; the noise rounding has been calculated by Ambegoakar and Halperin[4] and Vystavkin *et al.*[5] for the case $C=0$ (C is the capacitance of the junction). Subsequently, Kurkijärvi and Ambegoakar[6] and Voss[7] computed the case $C\neq 0$. Second, the fluctuations generate a voltage noise when the junction is current biased at a nonzero voltage. Likharev and Semenov[8] and Vystavkin *et al.*[5] showed that for the $C=0$ case in the limit $h\nu_J \ll k_BT$ ($\nu_J = 2eV/h$ is the Josephson frequency) and for frequencies much less than ν_J, the spectral density of the voltage noise is given by

$$S_v(0) = \frac{4k_BTR_D^2}{R}\left[1+\frac{1}{2}\left[\frac{I_0}{I}\right]^2\right]. \tag{1.1}$$

Here, R_D is the dynamic resistance. This result was derived on the assumption that the noise is sufficiently small that one can neglect departures of the I-V characteristic from that of the ideal RSJ,[1,2]

$$V = R(I^2 - I_0^2)^{1/2}. \tag{1.2}$$

Thus, Eq. (1.1) is not valid in the noise-rounded region $I < I_0$. Voss[7] and Koch and Clarke[9] computed the noise for the case $C\neq 0$. Experimental results are in good agreement with calculations for both the noise rounding[10] and voltage noise.[11]

For a junction voltage-biased on a self-resonant step, Stephen[12] has calculated the contribution of pair current fluctuations to the linewidth of the Josephson radiation. This noise arises from photon number fluctuations (including zero-point fluctuations) in the lossy cavity formed by the junction, and is not intrinsic to the tunneling of Cooper pairs in a nonresonant junction. Experimental re-

sults[13] are in good agreement with the predictions.

More recently, Koch *et al.*[14] considered the limit $h\nu_J \gtrsim k_B T$ in which quantum correction to the noise generated in the shunt resistor become important. The equation of motion for the junction is

$$\frac{\hbar C}{2e}\ddot{\delta}+\frac{\hbar}{2eR}\dot{\delta}+I_0\sin\delta=I+I_N\ , \tag{1.3}$$

where δ is the phase difference across the junction, and the noise current $I_n(t)$ has a spectral density[15]

$$S_i(\nu)=\frac{2h\nu}{R}\coth\left[\frac{h\nu}{2k_BT}\right]$$
$$=\frac{4h\nu}{R}\left[\frac{1}{\exp(h\nu/k_BT)-1}+\frac{1}{2}\right]. \tag{1.4}$$

In the limit[1,2] $0<\beta_c\equiv 2\pi I_0R^2C/\Phi_0\ll 1$ ($\Phi_0\equiv h/2e$), the first term on the left-hand side of Eq. (1.3) can be neglected, and the equations can then be solved analytically using the techniques of Likharev and Semenov.[8] At frequencies much less than ν_J and in the limit $I/I_0>1$, in which noise rounding can be neglected, the spectral density of the voltage noise $S_v(0)$ is given by

$$\frac{S_v(0)}{R_D^2}=\frac{4k_BT}{R}+\frac{2eV}{R}\left[\frac{I_0}{I}\right]^2\coth\left[\frac{eV}{k_BT}\right]. \tag{1.5}$$

The first term on the right-hand side is noise-generated at the measurement frequency, while the second term is noise-generated near the Josephson frequency that is mixed down to the measurement frequency by the nonlinearity of the junction. The contribution of noise-generated near frequencies $2\nu_J, 3\nu_J, \ldots$ is negligible in the ideal RSJ model.

Equation (1.5) reduces to Eq. (1.1) in the limit $eV\ll k_BT$. In the limit $eV\gtrsim k_BT$, quantum corrections to the mixed-down noise become important, and the second term will become comparable to the first term on the right-hand side of Eq. (1.5) when $eV(I_0/I)^2\gtrsim 2k_BT$. These requirements can be met provided $\kappa\gtrsim 1$, where

$$\kappa\equiv eI_0R/k_BT\ . \tag{1.6}$$

In the extreme quantum limit $eV\gg k_BT$, Eq. (1.5) reduces to

$$\frac{S_v(0)}{R_D^2}=\frac{2eV}{R}\left[\frac{I_0}{I}\right]^2 \tag{1.7}$$

and the observed noise is generated solely by zero-point fluctuations in the shunt resistor. In our picture, the resistor can be modeled as a large collection of harmonic oscillators. In the ground state at $T=0$, where there are no thermal fluctuations, the zero-point energy still induces fluctuations in the tilted periodic potential, thus generating a randomness in the rate at which the phase δ propagates.

This model also predicts "quantum activation," that is, a noise-rounding of the I-V characteristic of an overdamped junction ($\beta_c<1$) even at $T=0$ due to zero-point fluctuations. Although we cannot yet make any quantitative statements, we suspect this description will fail when I becomes significantly smaller than I_0. In this limit, transitions out of the zero-voltage state become very infrequent, and the model represented by Eq. (1.3) in which the particle is a point mass is likely to become invalid. Instead, one must treat the particle as a quantum-mechanical wave packet, which has some probability of penetrating the barrier by macroscopic quantum tunneling (MQT), as has been calculated by several authors.[16–19] Clearly, a quantitative theory that can deal with both zero-point fluctuations and MQT for all values of the bias current and damping is very much needed.

In this paper we describe measurements of the voltage noise in current-biased overdamped junctions ($\beta_c<1$) in the free-running mode $I>I_0$. In Sec. II we describe the experimental procedures and in Sec. III we present the experimental results and compare them with the predictions of the theory. Section IV contains some concluding remarks. An appendix outlines the procedure used in the computer modeling.

II. EXPERIMENTAL PROCEDURES

A. Junction fabrication

To observe quantum noise effects, we require junctions with $\kappa\gtrsim 1$. Writing

$$\kappa=(e/k_BT)(\beta_c\Phi_0 j_1/2\pi c)^{1/2}\ ,$$

where j_1 is the critical current density and c is the capacitance per unit area, we see that junctions with high critical densities are necessary to observe these effects in the liquid-^{4}He temperature range. At 4.2 K, with $\beta_c=0.2$, $j_1=10^4$ A cm^{-2}, and $c=0.04$ pF μm^{-2}, we find $\kappa\approx 1.1$.

Our junctions [Fig. 1(a)] were fabricated on glass substrates using photolithographic lift-off techniques.[20] We first deposited a 10-μm-wide Cu (0–3 wt % Al) film 40- to 100-nm thick and then a 10-μm-wide, 250-nm-thick Pb (20 wt % In) film.

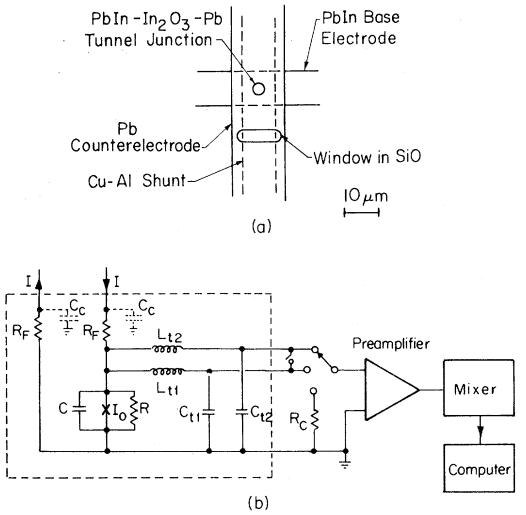

FIG. 1. (a) Configuration of resistively shunted tunnel junction; (b) schematic of measuring circuit; the dashed lines enclose the components immersed in liquid helium.

A SiO layer, 100-nm thick, was deposited and two windows were opened by lift-off to expose the PbIn and CuAl films. After patterning the resist for the upper electrode, the exposed metal surfaces were cleaned by rf sputter-etching in Ar, the In_2O_3 was grown thermally in a low pressure of oxygen, the 400-nm-thick Pb counter electrode was deposited and lifted-off, and a final protective layer of SiO was evaporated. The diameter of the junction was about 2.5 μm and its capacitance was about 0.5 pF (see Sec. III D). The critical current ranged from 0.1 to 2 mA at 4.2 K and the resistance of the shunt ranged from 0.05 to 0.7 Ω. The Pb counter electrode formed a ground plane for the shunt, reducing its inductance L_s to about 0.2 pH. Junctions fabricated with these techniques omitting the resistive shunts displayed excellent tunneling characteristics with little excess current at voltages below the sum of the gaps.

B. Measurement procedures

Each junction was immersed in liquid ^{4}He, and surrounded by a superconducting can and a *mu*-metal can. We measured the *I-V* characteristic and dynamic resistance and obtained the shunt resistance by reducing the critical current nearly to zero. The circuit for measuring the noise across a junction is shown in Fig. 1(b). The low-pass filters for the bias current consisted of a cooled 1.5-$k\Omega$ resistor R_F and the cable capacitance C_c. The two cooled LC-resonant circuits with inductors L_{t1}, L_{t2} and capacitors C_{t1}, C_{t2} had resonant frequencies of 70 and 183 kHz. Each tank circuit was connected in turn to a Brookdeal 5004 preamplifier; in addition, by connecting together the tank circuit leads we could measure the noise at a third, intermediate frequency, about 106 kHz. After further amplification, the noise was mixed-down to frequencies below 500 Hz and its spectral density was measured with a typical averaging time of 10 min. The system gain was calibrated against the Nyquist noise of a resistor R_c(5.1 $k\Omega$) to $\pm 2\%$. The noise produced by the junction across the tank circuit was $Q^2 S_v(0) = \omega^2 L_t^2 [S_v(0)/R_D^2]$, so that the required quantity $S_v(0)/R_D^2$ was independent of Q. We note that the predicted value of $S_v(0)/R_D^2$ is virtually independent of β_c in the range $0 < \beta_c \lesssim 0.5$, while the value of $S_v(0)$ does increase significantly as β_c is increased in this range.[7,9] Thus, for β_c appreciably greater than zero (junctions 2 and 3), it is more appropriate to compare experimental and theoretical values of $S_v(0)/R_D^2$ rather than $S_v(0)$.

We now discuss the various measured corrections to the noise spectral density.

(i) Corrections were made for the measured preamplifier voltage and current noise. The preamplifier noise was comparable with the junction noise at 4.2 K, and the corresponding error introduced by the correction was about $\pm 5\%$.

(ii) Noise due to losses in the tank circuit was negligible for the 70- and 183-kHz tank circuits, but not for the 106-kHz tank circuit, which contained leads that were partially at room temperature. In the last case, the error in the correction was $\pm 5\%$.

(iii) From measurements at three frequencies we determined that some junctions (2 and 4) generated a small amount of $1/f$ noise.[21] For example, for junction 2 at 183 kHz the $1/f$ noise was typically 10% or less of the white-noise spectral density at the higher voltages; even if the uncertainty in the noise was as high as $\pm 30\%$, the error introduced was no more than $\pm 3\%$.

(iv) The noise measurements were performed at bias voltages well below the sum of the gaps of the two superconductors. The quasiparticle current I_{qp} contributes a noise with a current spectral density[13] $2eI_{qp}\coth(eV/2k_BT)$. Thus, the ratio of the spectral densities of the quasiparticle and mixed-down noises is of order $I_{qp}/(V/R)$, which we estimate to be $\lesssim 10^{-2}$ at 4.2 K.

(v) The power dissipation in the shunt resistor

caused a significant temperature rise at the high bias voltages in some junctions. We determined the rise ΔT by reducing the critical current almost to zero and measuring the Nyquist noise of the shunt as a function of power dissipation. At low bias voltages the measured noise agreed with the Nyquist formula to within $\pm 3\%$. For most junctions the heating effect was important only at bias voltages $V \gg k_B T/e$, where the mixed-down term in Eq. (1.5) is nearly independent of the shunt temperature. Thus, it was sufficient to correct the data by subtracting $4k_B \Delta T/R$ from the measured noise; the maximum error introduced was $\pm 3\%$. However, for junction 3, where the heating correction was particularly large, it was necessary to correct the mixed-down term was well.

(vi) We took considerable care to shield the experiment from extraneous noise sources, and to avoid coupling significant 300-K noise into the low-temperature circuitry. Measurement of the Nyquist noise in cooled resistors were within $\pm 3\%$ of the predicted value, and measurements on junctions in the classical limit $eV \ll k_B T$ showed the correct temperature dependence and were in excellent agreement with theory (see Secs. III A, III B, and III C). Thus, we believe our measurements were not significantly influenced by extraneous noise sources.

III. EXPERIMENTAL RESULTS AND COMPARISON WITH THEORY

We report results on four different junctions that illustrate various aspects of the theory. The essential parameters of the junctions are listed in Table I.

A. Junction 1

As a test of our measurement system and of the effectiveness of the shielding we first investigated a junction in the limit $\kappa \ll 1$ in which the Likharev-Semenov[8] result, Eq. (1.1), is applicable. At 4.2 K, the value of κ was 0.066. The parameters β_c and $\beta_L \equiv 2\pi L_s I_0/\Phi_0$ were 0.003 and 0.2, respectively, so that the I-V characteristic was very close to that for an ideal resistively shunted junction (see Sec. IV D for a discussion of the effects of the value of β_L). The $1/f$ and heating corrections were negligible through the range of measurement, so that the only corrections to the measured data were for preamplifier and tank circuit noise. (In this experiment, the measurements were at two frequencies only, 30 and 100 kHz.) In Fig. 2 we compare the measured noise with the predictions of Eq. (1.1). In plotting the theoretical points we used the predicted dynamic resistance[1,2]

$$R_D = R\left[1 - I_0^2/I^2\right]^{-1/2}, \tag{3.1}$$

so that only the measured values of R, I_0, I, and T were used. Thus, we have neglected noise rounding,[4] and the predicted spectral density of the noise diverges as $I \to I_0$. Above the noise-rounded region, the agreement between theory and experiment is very good indeed. At very low voltages, the measured noise decreases as the current is lowered because the noise-rounded dynamic resistance decreases. The good agreement between theory and

TABLE I. Parameters of junctions. $C = 0.5$ pF for 1,2,3; 0.81 pF for 4. $L = 0.2$ pH for 1,2,3; 0.23 pH for 4; the value of R at 100 μV was used to compute β_c and κ.

Junction	1	2		3	4
Temperature (K)	4.2	4.2	1.6	4.2	1.4
I_0 (mA)	0.32	0.51	0.60	0.36	1.53
R (Ω)	0.075	0.67 Ω at 50 μV 0.70 Ω at 100 μV 0.75 Ω at 400 μV		0.58 Ω at 50 μV 0.62 Ω at 100 μV 0.68 Ω at 200 μV 0.77 Ω at 400 μV	0.084 Ω at 50 μV 0.092 Ω at 100 μV
β_c	0.003	0.38	0.45	0.21	0.032
β_L	0.20	0.31	0.37	0.22	1.05
κ	0.066	0.99	3.0	0.62	1.17
$S_I^{1/f}$ ($A^2 Hz^{-1}$)	$<2\times10^{-22}$	6.0×10^{-23}	3.0×10^{-23}	$<3\times10^{-24}$	5.5×10^{-22}
Frequency	100 kHz	183 kHz	183 kHz	183 kHz	100 kHz
Heating (K/μW)	<1	0.25	1.6	7	1.6

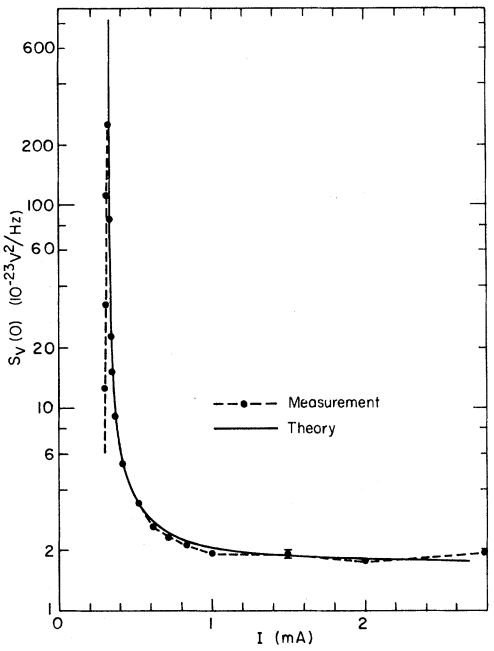

FIG. 2. $S_v(0)$ vs I for junction 1 at 4.2 K. Solid circles are data with dashed line drawn through them; solid line is prediction of Eq. (1.1).

experiment for $I > I_0$ indicates very strongly that the contribution of extraneous noise sources is negligible.

B. Junction 2

The parameters of this junction (Table I) were chosen to emphasize the quantum effects: Thus κ increased from 0.99 at 4.2 K to 3.0 at 1.6 K (the critical current increased slightly as the temperature was lowered). The values of β_c and β_L, about 0.38 and 0.31 at 4.2 K, respectively, were small enough that the deviations from the ideal resistively shunted junction were relatively minor. Figure 3 shows I and dV/dI vs V at 4.2 K. There is a small drop in dV/dI at about 800 μV which we believe is associated with a resonance of the shunt inductance and the junction capacitance (see Sec. III D). There is also some very fine structure and a dip at 300 μV of unknown origin. We emphasize that in comparing the quantity $S_v(0)/R_D^2$ with the theory, small deviations in R_D from Eq. (3.1) will be suppressed provided the mixing coefficient $(I_0^2/2I^2)$ in Eq. (1.5) is not affected by the additional nonlinearity. Another deviation from the simple model arose because the shunt resistance R which was measured with the critical current

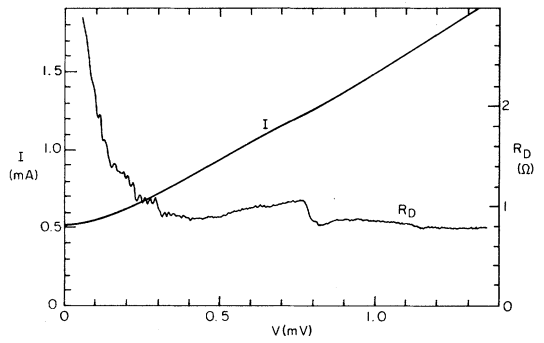

FIG. 3. I and R_D vs V for junction 2 at 4.2 K.

suppressed nearly to zero, varied between 0.65 and 0.75 Ω as the voltage bias was increased from 0 to 1 mV. We believe this variation was the result of a proximity effect between the shunt and the electrodes or possibly of diffusion of Pb into the shunt. The measured value of R was used at each voltage bias when we compared theory and experiment.

In Fig. 4 we plot measured values of $S_v(0)/R_D^2$ versus voltage (open circles) after the preamplifier noise has been subtracted. The solid circles are the noise after the $1/f$ noise subtraction and the heating correction have been made. At low voltages the correction is entirely due to $1/f$ noise, while at high voltages the correction is largely due to heating. In the mid-voltage range, both corrections are small. The solid line through the solid circles is the prediction of Eq. (1.5) using the measured values of R, I_0, I, V, and T. The upper dashed line is the predicted noise in the absence of zero-

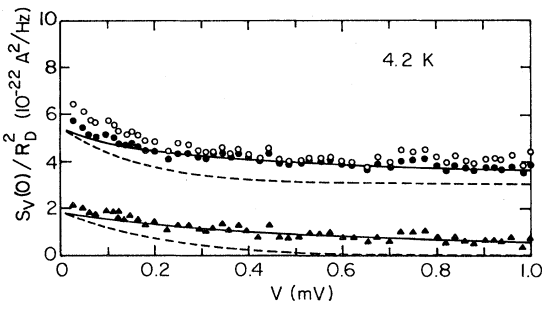

FIG. 4. $S_v(0)/R_D^2$ at 183 kHz vs V for junction 2 at 4.2 K. The open circles show the total measured noise across the junction; solid circles below show the noise remaining after correction for $1/f$ noise and heating. Upper solid and dashed lines are predictions of Eq. (1.5) and (3.2). Solid triangles are measured mixed-down noise, lower solid and dashed lines are mixed-down noise predicted by Eqs. (1.5) and (3.2).

point fluctuations, that is

$$\frac{S_v'(0)}{R_D^2}=\frac{4k_BT}{R}+\frac{4eV}{R}\left[\frac{I_0}{I}\right]^2\frac{1}{\exp(2eV/k_BT)-1}\ . \tag{3.2}$$

The triangles in Fig. 4 represent the measured mixed-down noise, which was computed by subtracting $4k_BT/R$ from the solid circles. The solid line through the triangles is the mixed-down noise predicted by Eq. (1.5),

$$(2eV/R)(I_0/I)^2\coth(eV/k_BT)\ ,$$

while the lower dashed line is the mixed-down noise predicted by Eq. (3.2) in the absence of zero-point fluctuations,

$$(4eV/R)(I_0/I)^2[\exp(2eV/k_BT)-1]^{-1}\ .$$

The small discrepancies between the data and Eq. (1.5) at very low voltages are possibly due to our neglect of noise rounding in the theory. It is evident from Fig. 4 that both the total measured noise across the junction and the measured mixed-down noise are in excellent agreement with the theory that includes a contribution from the mixed-down zero-point fluctuations, and are substantially higher than the predictions of a theory that does not include this contribution.

In Fig. 5 we show the temperature dependence of the noise for twelve bias voltages ranging from 50 to 550 μV. The notation is the same as that in Fig. 4. The temperature $T=2eV/k_B$ is indicated for the six lowest voltages; mixed-down noise at temperatures well above this temperature is in the classical limit $eV\ll k_BT$, while that at temperatures well below this temperature is in the quantum limit $eV\gg k_BT$. The mixed-down noise at the six highest voltages is in the quantum limit at all temperatures measured. For all twelve voltages, the total junction noise is in good agreement with the predictions of Eq. (1.5) and substantially greater than the predictions of Eq. (3.2). The data at 300 μV, however, lie somewhat above the prediction. This discrepancy arises from the structure at 300 μV (see Fig. 3) that increases the magnitude of the mixed-down noise above the value predicted by Eq. (1.5) (this topic will be discussed in detail in Sec. III D). The mixed-down noise at 350 μV and above is independent of temperature, and in excellent agreement with the value of Eq. (1.7),

$$S_v(0)/R_D^2=(2eV/R)(I_0/I)^2\ .$$

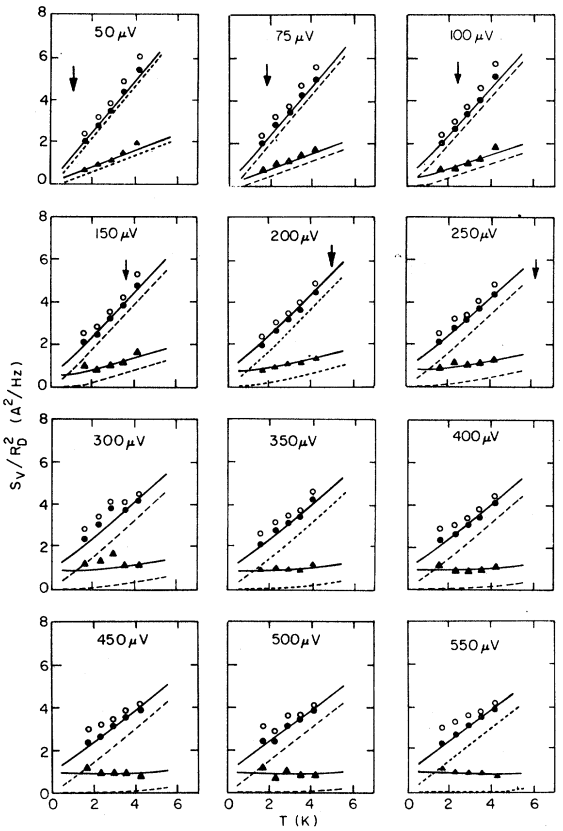

FIG. 5. $S_v(0)/R_D^2$ at 183 kHz vs T for junction 2 at 12 bias voltages. Notation is as for Fig. 4. Arrows indicate $2eV=k_BT$.

(As the temperature was lowered, I_0 increased slightly, giving rise to the slight increase in the mixed-down noise that is evident in both the data and the theoretical prediction.) As the voltage is lowered the mixed-down noise becomes increasingly temperature dependent, and remains in good agreement with the predictions of Eq. (1.5). At 50 μV, the mixed-down noise is in the classical limit for the whole temperature range and proportional to T as expected. This temperature dependence demonstrates that the contribution of any extraneous noise was negligible.

We can extract from our data the measured spectral density of the current noise $S_I(\nu)$ generated by the shunt resistance R at the Josephson frequency $\nu=2eV/h$. We divide each value of the mixed-down noise by the mixing coefficient $(I_0/I)^2/2$, a procedure that converts the mixed-down noise in Eq. (1.5) into Eq. (1.4). The results are plotted in Fig. 6 for 4.2 K (solid circles) and 1.6 K (open circles). The solid lines are the corresponding predictions of Eq. (1.4) using measured

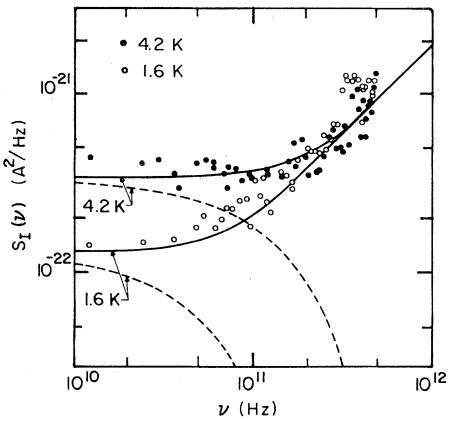

FIG. 6. Measured spectral density of current noise in shunt resistor of junction 2 at 4.2 K (solid circles) and 1.6 K (open circles). Solid lines are prediction of Eq. (1.4), while dashed lines are $(4h\nu/R)[\exp(h\nu/k_BT)-1]^{-1}$.

values of $\nu=2eV/h$, R, and T. The slight increase of the data above the theory at the highest voltages may reflect the presence of a resonance on the I-V characteristic. The agreement between the data and the predictions is rather good, bearing in mind that, once again, no fitting parameters are used. By contrast, the dashed lines represent the theoretical prediction in the absence of the zero-point term,

$$(4h\nu/R)[\exp(h\nu/k_BT)-1]^{-1},$$

and fall far below the data at the higher frequencies. The existence of zero-point fluctuations in the measured spectral density of the current noise is rather convincingly demonstrated.

C. Junction 3

An alternative means of varying the mixed-down noise between the quantum and thermal limits is to change I_0 at fixed temperature. The critical current was lowered by trapping flux in the junction. The $1/f$ noise in junction 3 at 183 kHz was insignificant ($<2\%$), but the heating correction at the higher voltages was substantial, so that it was necessary to correct the mixed-down noise in addition to the noise generated at the measurement frequency. In Fig. 7 we plot $S_v(0)/R_D^2$ vs V at 4.2 K for four values of I_0 corresponding to values of κ ranging from 0.65 to 0.07. At the highest two values of I_0, the presence of a resonance near 200 μV increased the magnitude of the measured noise

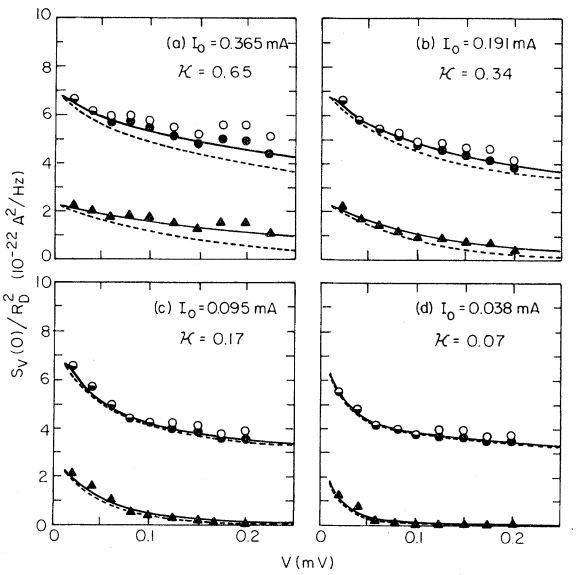

FIG. 7. $S_v(0)$ at 183 kHz vs V for junction 3 at 4.2 K for four values of I_0. Notation is as for Fig. 4.

somewhat above the prediction of Eq. (1.5). Apart from this discrepancy, the measured total noise and the measured mixed-down noise are in very good agreement with the predictions. For $\kappa=0.65$, the data lie convincingly above the theory that does not include the mixed-down zero-point fluctuations, while for $\kappa=0.07$ the contribution of the zero-point term is less than our experimental error. Once again, the correct observed dependence of the noise on I_0 demonstrates the absence of any significant extraneous noise.

D. Junction 4

As noted earlier, some junctions contain resonances that can effect the magnitude of the noise mixed-down to the measurement frequency. Junction 4 exhibited strong resonant structure, and we have investigated its origin and its effect on the noise in some detail. Figure 8 shows the I-V and (dV/dI)-V characteristics at 1.1 K for four values of critical current; the three lowest values were obtained by trapping flux in the junction. The structure arises from the resonant circuit formed by the shunt inductance L_s and junction capacitance C; the equivalent circuit is shown in the inset in Fig. 9. The resonant circuit pulls the Josephson frequency slightly so that it become more closely a subharmonic of the resonant frequency. Hence, as the current bias is increased, the dynamic resis-

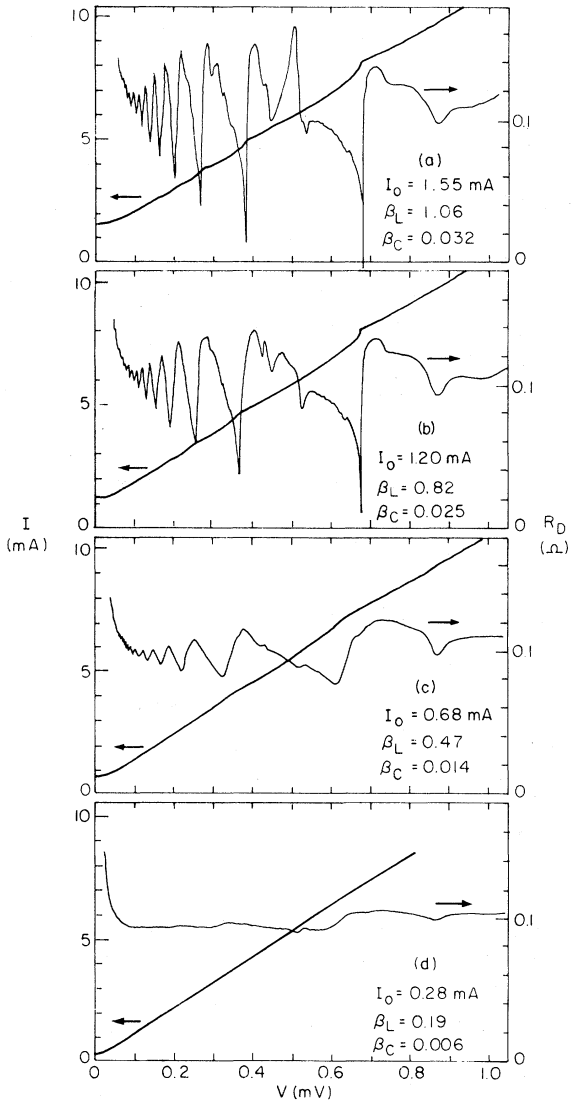

FIG. 8. *I-V* and dV/dI-*V* curves for junction 4 at 1.1 K for four values of I_0.

tance will be alternately increased and decreased as the Josephson frequency passes through each subharmonic frequency of the *LCR* resonance. The $1/n$ dependence of the dynamic resistance is shown clearly in Figs. 8 and 9 (n is an integer).

The equations of motion are

$$I = I_0 \sin\delta + C\dot{V} + I_s \tag{3.3}$$

and

$$V = I_s R + \dot{I}_s L_s + V_N \ , \tag{3.4}$$

where I_s is the current flowing through the shunt and V_N is the equilibrium noise voltage generated

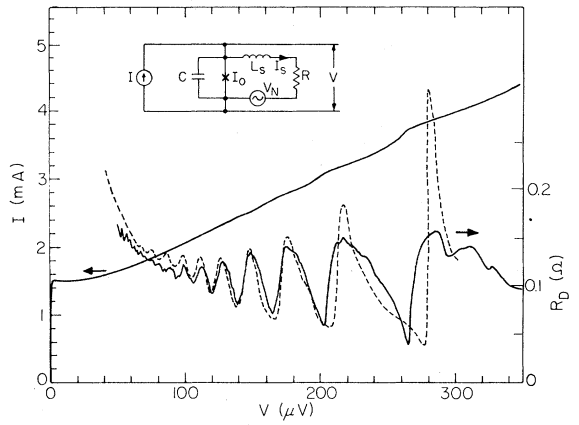

FIG. 9. I and R_D vs V for junction 4 at 1.4 K with $I_0 = 1.53$ mA, $R = 0.092$ Ω, $\kappa = 1.17$, $\beta_L = 1.05$, and $\beta_c = 0.032$. Dashed line is computed R_D. Inset is equivalent circuit of junction.

by R with spectral density $2h\nu R \coth(h\nu/2k_BT)$. We have computed the *I-V* characteristics and the spectral density of the voltage noise across the junction, using the procedure outlined in the Appendix. To obtain these curves, it was necessary to fit the values of L_s and C. From our simulations, we conclude that the *I-V* characteristic will show substantial resonant structure when $\beta_L = 2\pi L_s I_0/\Phi_0 \gtrsim 0.5$ and the approximate Q of the *LCR* circuit $(\beta_L/\beta_C)^{1/2} \gg 1$. The observed rapid decrease in the magnitude of the resonant structure as I_0 is lowered is demonstrated in Fig. 8.

Figure 9 shows I and R_D vs V for junction 4 at 1.4 K, the temperature at which the noise measurements were made. The computed dynamic resistance is also shown, using $L_s = 0.23$ pH and $C = 0.81$ pF; these values are consistent with values expected from the dimensions of the sample. The agreement between the measured and computed values is quite good, although the measured structure at the higher voltages is considerably more smeared than predicted, possibly because of noise rounding. Furthermore, the measurements lie slightly below the computed values at lower voltages, even though noise rounding is negligible in this region. This discrepancy occurs because the measured shunt resistance at low voltages dropped somewhat below the high-voltage value, a fact that could not readily be included in the computer simulation (see Appendix).

This junction was investigated at an early stage of our work, and we measured the noise mostly at one frequency only, 98.6 kHz, with a few measure-

ments at 31.6 kHz. We used the following procedure to subtract the $1/f$ noise in the range of voltage where the oscillations occurred. First, if the $1/f$ noise arises from fluctuations in the critical current,[21] the spectral density of the voltage noise should be proportional to $(\partial V/\partial I_0)^2$. At voltages where the RSJ result, Eq. (1.2), is valid we find

$$\left[\frac{\partial V}{\partial I_0}\right]^2 = R^2\left[\frac{I_0 R}{V}\right]^2 . \tag{3.5}$$

Hence, the voltage noise arising from $1/f$ fluctuations will be

$$S_v^{1/f}(\nu) = R^2(I_0R/V)^2 S_{I_0}^{1/f}(\nu) , \tag{3.6}$$

where $S_{I_0}^{1/f}(\nu)$ is the spectral density of the $1/f$ fluctuations in the critical current at the measurement frequency. Second, the mixed-down noise in Eq. (1.1) for voltages well below k_BT/e can be written as $(2k_BTR)(I_0R/V)^2$. Thus, at low voltages where the deviations from the RSJ model are negligible and for fixed values of I_0, R, and T, the spectral densities of both the mixed-down noise and $1/f$ noise (and their sum) should be proportional to $1/V^2$. Figure 10 shows the spectral densities of the voltage noise across the junction for $V < 100$ μV at 98.6 kHz and for two voltages at 31.6 kHz, with the direct term $(4k_BT/R)R_D^2$ subtracted out. At 98.6 kHz the plotted quantity

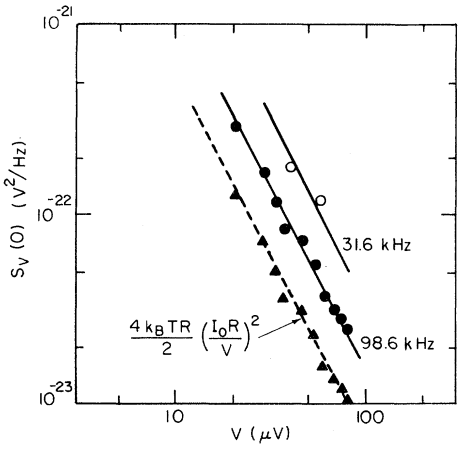

FIG. 10. Spectral density of total voltage noise across junction 4 at two frequencies in the region $V < k_BT/e$ with $(4k_BTR_D^2/R)$ subtracted out (open and solid circles). Solid lines have slope -2. Triangles are measured mixed-down noise assuming excess low-frequency noise is proportional to $1/f$; dashed line is prediction of Eq. (1.1).

scales with $1/V^2$, suggesting that the $1/f$ noise scales as $(\partial V/\partial I_0)^2$. We then assume that the spectral density of the excess noise scales as $1/f$ and from data at the two voltages where measurements were made at two frequencies we calculate the spectral density of the $1/f$ noise in the critical current: $S_{I_0}^{1/f}(98.6\text{ kHz}) = 5.5\times10^{-22}\text{ A}^2\text{Hz}^{-1}$. By subtracting the $1/f$ voltage noise computed using Eq. (3.6) from the data at 98.6 kHz, we obtain the mixed-down noise shown in Fig. 10. The mixed-down noise is in excellent agreement with the predicted value. Thus, this procedure provides strong evidence that the spectral density of the excess noise at low voltages scales closely as $1/f$ (as is the case for all junctions on which we have measurements at three frequencies). We then calculated the $1/f$ voltage noise at higher voltages (> 100 μV) from measurements at 98.6 kHz using the value of $S_{I_0}^{1/f}$ quoted above, together with measured values of $\partial V/\partial I_0$. We also measured the noise at 31.6 kHz at several voltages between 100 and 200 μV and obtained values that were consistent with those obtained by the above procedure. Since the overall $1/f$ correction was small, typically 15% or less of the total junction noise at 200 μV, we believe that the error introduced by the correction is at most $\pm5\%$ of the mixed-down noise.

As a further complication, we did not measure the heating correction on this junction, but rather on one fabricated simultaneously. As a result the heating correction had a higher uncertainty, which we estimate to be $\pm6\%$ of the total spectral density, than for the other junctions.

Figure 11(a) shows the spectral density of the measured voltage noise at 1.4 K, together with the measured mixed-down noise computed by subtracting $4k_BTR_D^2/R$, with the $1/f$ noise subtracted. The solid line shows the result of the computer simulation, with the zero-point term included and with the values of L_s and C obtained by fitting the model to the I-V characteristics in Fig. 10. The data tend to lie somewhat above the computed curve at voltages above 100 μV. In Fig. 11(b) we have applied a heating correction by subtracting $4k_B\Delta TR_D^2/R$ from the solid circles in Fig. 11(a). The agreement between the measured and computed values is now rather good, indicating that our model is a good approximation.

Our computer simulation yields the magnitudes of the contributions of the noise generated at multiples of the Josephson frequency as shown in Fig. 12. We define a mixing impedance[8] Z_k via the re-

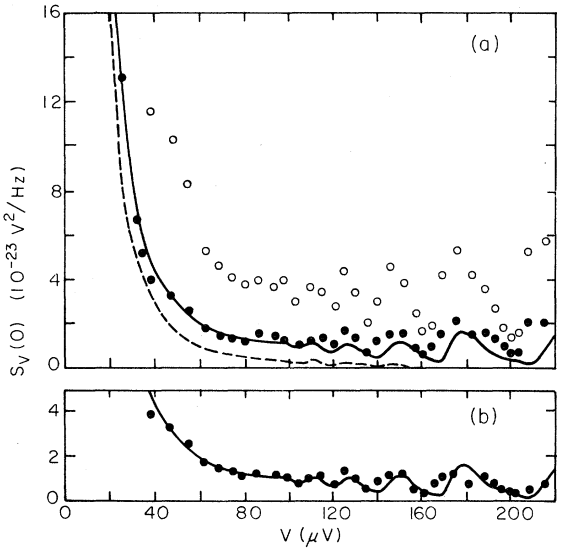

FIG. 11. (a) Open circles are measured voltage noise at 100 kHz across junction 4 at 1.4 K; solid circles are mixed-down noise with $1/f$ noise subtracted. Solid and dashed lines are predictions of computer simulation with and without zero-point term. (b) Solid circles are data after heating correction has been made, solid line is identical to that in (a).

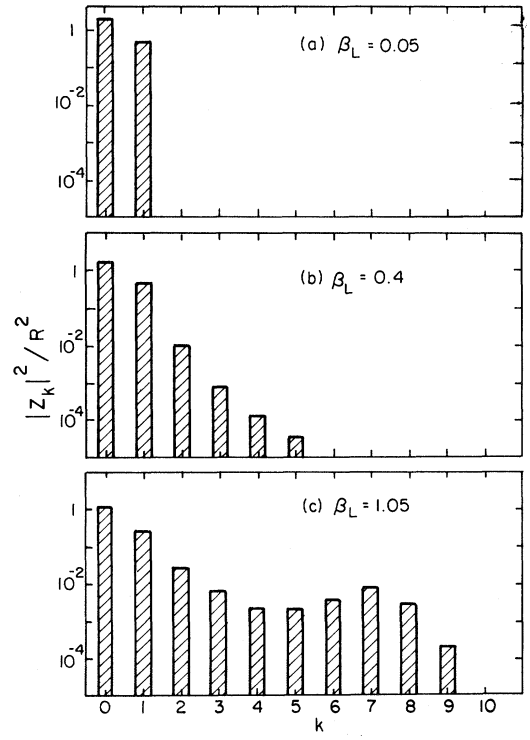

FIG. 12. $|Z_k|^2/R^2$ for a junction with $\beta_c=0.031$ for three values of β_L and a bias current $I/I_0=1.42$.

lation (see the Appendix)

$$S_v(0)=\sum_{k=0}^{\infty} S_v^{(k)}(0)=\sum_{k=0}^{\infty} |Z_k|^2 S_I(k\nu_J)\,, \tag{3.7}$$

where $k=0, 1, 2, \ldots$ and $S_v^{(k)}(0)$ is the spectral density of the mixed-down voltage noise due to noise near frequency $k\nu_J$. We note that $|Z_0|^2=R_D^2$. For $\beta_c=0.031$ and $\beta_L=0.05$, Z_k is essentially zero for $k\geq 2$, and the deviations from the RSJ model are negligible. On the other hand, for $\beta_L=0.4$ and 1.05, there are very substantial contributions to the noise from harmonics out to the fifth and ninth, respectively, and the noise is considerably enhanced over the value predicted by Eq. (1.5). These results explain quantitatively the additional noise associated with the resonant structure, and qualitatively, the additional noise observed on junctions 2 and 3 in the vicinity of structure on the I-V characteristic. In fact, the capacitance and inductance of these two junctions were estimated from computer fits to this structure.

Although the data obtained from junction 4 are considerably harder to interpret than those from the other junctions, the role of zero-point fluctuations is even more important because of the large number of harmonics that contribute to the mixed-down noise. The noise generated at frequencies near the higher harmonics can be in the quantum limit even for junctions with $\kappa<1$.

IV. CONCLUDING REMARKS

We emphasize that in comparing the data for junctions 1, 2, and 3 with theory we have used only measured parameters; there is no fitting of the data. Thus, junctions 2 and 3 provide the main evidence for the accuracy of Eq. (1.5). We believe the results obtained from these junctions are a convincing demonstration; first of the existence of a zero-point term is the spectral density of the current noise of a resistor in thermal equilibrium (Fig. 6), and second, evidence that these fluctuations give rise to the limiting voltage noise in a current-biased resistively shunted Josephson junction in the quantum limit for $I>I_0$ (Figs. 4, 5, and 7). Furthermore, the good agreement between our results and Eq. (1.5) justifies our use[14] of a Langevin equation together with a zero-point driving term to predict quantum noise effects in a current-biased Josephson junction in the overdamped limit when it is in the free-running mode $I>I_0$. We were not able to examine the validity

of the theory in the noise-rounded case $I < I_0$ since quantum effects are negligible in this regime in the ^{4}He temperature range for the parameters of our junctions.

The data from junction 4, which exhibited resonant structure, require a fitting of L_s and C to compare the experimental results with the theory. However, we note that the values of L_s and C that yield an excellent fit to the measured I and dV/dI vs V characteristics, also produce a very good fit to the noise data (Fig. 11). These results show very dramatically the strong effects of additional nonlinearities on the voltage noise due to the mixing-down of higher-order harmonics. Because quantum effects increase rapidly as the order of the harmonic increases, the role of zero-point fluctuations is even more pronounced in junctions with resonant structure.

The fact that the zero-point fluctuations in the resistor can be observed at frequencies as high as 5×10^{11} Hz implies that a Josephson mixer using the ac Josephson effect as the local oscillator is an ideal quantum-limited device at these frequencies. When an external local oscillator is used, however, the additional nonlinearity induced on the I-V characteristic causes noise near the higher harmonics of the Josephson frequency to be mixed-down, thereby greatly increasing the noise of the mixer. This limitation of the Josephson mixer with an external local oscillator has been discussed extensively by other authors.[22,23]

Finally, in accord with other observations,[24,25] we find no evidence for a contribution to the measured noise arising from the shot noise of pairs tunneling through the junction. For example, in Fig. 4, the spectral density of a term $4eI_0$ would be about 3.2×10^{-22} A^2 Hz^{-1}, a value at least five times greater than the observed mixed-down noise at 1 mV. We emphasize, however, this this observation in no way invalidates the theory of Stephen,[12] which is applicable to a quite different situation.

ACKNOWLEDGMENTS

R. H. Koch and D. J. Van Harlingen would like to thank the National Science Foundation for pre- and post-doctoral fellowships. We should like to thank Dr. J. H. Greiner and Dr. L. D. Jackel and his colleagues for helpful discussions on junction fabrication. We are indebted to the Micro Electronics Facility in the Electronics Research Laboratory of the Electrical Engineering and Computer Science Department at the University of California at Berkeley for the use of their facilities. This work was supported by the Director, Office of Energy Research, Office of Basic Energy Sciences, Materials Sciences Division of the U.S. Department of Energy, under Contract No. W-7405-ENG-48.

APPENDIX: TWO METHODS OF COMPUTING I-V CHARACTERISTICS AND NOISE IN RESISTIVELY SHUNTED JUNCTIONS

In this appendix, we outline two methods of computing the I-V characteristics and spectral density of the voltage noise for resistively shunted junctions. The first method calculates the I-V characteristics and R_D, including noise-rounding, and can also be used to compute the spectral density of the voltage noise, although the last calculation is rather slow. Unfortunately, for reasons that we will explain, this method is not useful for computing the noise in a junction with resonant structure, such as junction 4. The second method calculates the noise very efficiently at voltages where noise rounding is negligible. With the model of the junction we have used, this method appears to account for most of the data observed on junction 4 satisfactorily, although higher-order corrections might provide a better fit at voltages above, for example, 500 μV.

1. Method 1

The model circuit, inset in Fig. 9, is described by Eqs. (3.3) and (3.4). We rewrite these equations in dimensionless units $v=V/I_0R$, $i=I/I_0$, $s=I_s/I_0$, and $\theta=t/(\Phi_0/2\pi I_0R)$:

$$i=\sin\delta+\beta_c\ddot{\delta}+s \tag{A1}$$

and

$$\dot{\delta}=s+\beta_L\dot{s}+v_n\ , \tag{A2}$$

where $\dot{\delta}\equiv\partial\delta/\partial\theta$, etc., and we have used $2eV=\hbar\partial\delta/\partial t$. As usual, $\beta_c\equiv2\pi I_0R^2C/\Phi_0$ and $\beta_L\equiv2\pi L_sI_0/\Phi_0$. The instantaneous state of the junction is specified completely by $\dot{\delta}$, δ, and s. Using Eqs. (A1) and (A2) one can compute $\dot{s}$ and $\ddot{\delta}$ and the higher-order derivatives. We have neglected all derivatives of v_n. Once the derivatives have been evaluated numerically for the existing values of δ, $\dot{\delta}$, and s at the time θ, we compute the new values δ_1, $\dot{\delta}_1$, and s_1 at a later time, $\theta+\tau$, by using

a fifth-order Taylor expansion. To predict the average voltage for $i>1$, we set $v_n=0$, integrate Eqs. (A1) and (A2) numerically over exactly one Josephson cycle, measure the required time θ_J, and compute $\langle v\rangle=\langle\dot{\delta}\rangle=2\pi/\theta_J=\omega_J$. This procedure was used to compute the values of R_D in Fig. 9, with values of L_s and C chosen to fit the data.

The results were independent of the length of the time step τ provided τ was less than the smaller of β_c or β_L. To check that the presence of noise did not affect the characteristics for $i>1$, we varied v_n in time to simulate noise from the resistor while the junction was allowed to evolve over many Josephson cycles. The resulting values of the voltage were identical to those with $v_n=0$.

To obtain a time representation of $v_n(\theta)$ with a white power spectrum, $S_v^{\rm w}(\omega)$ (ω is the dimensionless angular frequency), we used a pseudo-random-number generator to produce voltage pulses that were Gaussian-distributed in amplitude and uncorrelated in time. A nonwhite power spectrum $S_v^{\rm nw}(\omega)$ could be generated, when necessary, by convolving this time representation with an appropriate filter function. This filter function was chosen so that its transfer function in the frequency domain $T(\omega)$ satisfied

$$S_v^{\rm nw}(\omega)=|T(\omega)|^2 S_v^{\rm w}(\omega)\ . \tag{A3}$$

The high-frequency cutoff, ω_H, of $v_n(\theta)$ was always chosen to be large enough that the predicted average voltage and noise voltage were independent of the value of ω_H when the latter was varied over a factor of 20 or more. Furthermore, when the noise near the Josephson frequency was nonwhite, we took account of the implied nonzero correlation time by ensuring that the correlation time of the filter was much larger than $1/\nu_J$.

To obtain $\langle\dot{\delta}\rangle$, the computer values of $\dot{\delta}(\theta)$ were filtered with a low-pass Gaussian filter with a roll-off frequency ω_L of 0.03 to $0.1\omega_J$. The fluctuations in the filtered values of $\langle\dot{\delta}\rangle$ were used to compute the low-frequency spectral density of the voltage noise. This spectral density was independent of the roll-off frequency of this low-pass filter.

This method was used in two earlier papers[15,26] to predict $\langle\dot{\delta}\rangle$ and the fluctuations in δ in single junctions and dc superconducting quantum interference devices (SQUID's), including low-voltage regions of the I-V characteristics where there is significant noise-rounding. However, when we tried to use this method to predict the noise in junction 4, which has substantial resonant structure, we obtained very poor results. The essential problem was that the resonant frequency, $\omega_{LC}=(L_sC)^{-1/2}$, was typically 5 to 20 times higher than ω_J, while ω_H was necessarily at least several times greater than ω_{LC}. Thus, since ω_L was typically an order of magnitude less than ω_J, the ratio of ω_H/ω_L was typically 10^3. Consequently, the ratio of the "input" noise power to the "output" noise power for "f noise" was typically 10^6. The computed spectral densities of the noise proved to be erratic with such large ratios, possibly because of our neglect of the derivatives of v_n. As a result, we had to abandon this technique for junctions with resonant structure.

2. Method 2

Above the noise-rounded region of the I-V characteristic, we used a more accurate but more complicated method to calculate the noise in resonant junctions. In this region, following the perturbation approach of Likharev and Semenov,[8] we can expand δ and s:

$$\delta(\theta)=\delta_0(\theta)+\tilde{\delta}(\theta) \tag{A4}$$

and

$$s(\theta)=s_0(\theta)+\tilde{s}(\theta)\ , \tag{A5}$$

where δ_0 and s_0 are the noise-free solutions for the phase and shunt current, and $\tilde{\delta}$ and $\tilde{s}$ represent small departures from δ_0 and s_0 due to noise. Substituting these expressions into Eqs. (A1) and (A2), we find

$$0=\tilde{\delta}\cos\delta_0+\beta_c\ddot{\tilde{\delta}}+\tilde{s} \tag{A6}$$

and

$$\dot{\tilde{\delta}}=\tilde{s}+\beta_L\dot{\tilde{s}}+v_n\ . \tag{A7}$$

We Fourier-transform these equations over the range $-\infty<\omega<\infty$ to obtain

$$0=\int_{-\infty}^{\infty}F(\omega')\tilde{\delta}(\omega-\omega')d\omega'+\beta_c(-\omega^2)\tilde{\delta}(\omega)+\tilde{s}(\omega) \tag{A8}$$

and

$$j\omega\tilde{\delta}(\omega)=(1+j\omega\beta_L)\tilde{s}(\omega)+v_n(\omega)\ , \tag{A9}$$

where $F(\omega')$ is the normalized Fourier transform of $\cos\delta_0(\theta)$. Since $\cos\delta_0(\theta)$ is a periodic function, $F(\omega')$ consists of a series of spiked functions centered at $\omega=0$ and spaced at intervals of ω_J. Setting $\omega'=k\omega_J$, where k is an integer, we can

transform the integral to a sum, replace $F(k\omega_J)$ with F_k, and eliminate s between Eqs. (A8) and (A9) to find

$$\sum_{k=-\infty}^{\infty} F_k \tilde{\delta}(\omega - k\omega_J) + \left[\frac{j\omega}{1+j\omega\beta_L} - \omega^2\beta_c \right] \tilde{\delta}(\omega) = \frac{v_n(\omega)}{1+j\omega\beta_L} . \quad \text{(A10)}$$

In subsequent calculations, we have shown that there exists a maximum value of $|k|$, k_m, above which the noise at frequency $k\omega_J$ is not significantly mixed-down to the measurement frequency. Cutting off the summation at $\pm k_m$, we are left with $2k_m + 1$ inhomogeneous equations with unknown phases $\tilde{\delta}(\omega - l_m\omega_J), \ldots, \tilde{\delta}(\omega + l_m\omega_J)$, where $|l| \leq k_m$. To solve these, we first compute the coefficients F_k using method 1 (with $v_n = 0$). The required fluctuations in the $\tilde{\delta}(\omega - l\omega_J)$ are then obtained by a conventional matrix inversion of Eq. (A10). We find

$$\tilde{\delta}(\omega + l\omega_J) = \sum_{k=-k_m}^{+k_m} \frac{A_{l,k} v_n(\omega + k\omega_J)}{1+j(\omega+k\omega_J)\beta_L} , \quad \text{(A11)}$$

where $\underline{A} \equiv \underline{B}^{-1}$, and $\underline{B}$ is the matrix representation of Eq. (A10):

$$\{\underline{B}\}_{l,k} = F_{l-k} + \delta_{l,k} \left[\frac{j(\omega+l\omega_J)}{1+j(\omega+l\omega_J)\beta_L} - (\omega+l\omega_J)^2\beta_c \right] . \quad \text{(A12)}$$

In Eq. (A12), $\delta_{l,k}$ is the Kronecker delta. Since the v_n at different frequenices are independent, the noise at the measurement frequency can be obtained from Eq. (A11) with $|\omega| \ll |\omega_J|$ and $l = 0$:

$$s_{\tilde{\delta}}(\omega) = \sum_{k=-k_m}^{k_m} |z_k(\omega)|^2 s_i(\omega + k\omega_J) , \quad \text{(A13)}$$

where

$$z_k(\omega + l\omega_J) = \frac{j(\omega+l\omega_J)A_{l,k}}{1+j(\omega+k\omega_J)\beta_L} , \quad \text{(A14)}$$

is the complex dimensionless impedance that mixes noise from $\omega + k\omega_J$ to $\omega + l\omega_J$, and $s_i(\omega + k\omega_J)$ is the dimensionless spectral density of the noise current in the resistor. We obtain Eq. (3.7) from Eq. (A13) by replacing ω with ν, setting $\nu = 0$, using positive frequencies only, and assigning appropriate dimensions. In dimensioned units, at frequencies small compared with Z_0/L_s, Z_0 is just the dynamic resistance. Thus, the method can be tested by comparing the value of Z_0 with the value of R_D obtained with method 1. The computed values of $z(\omega)$ were shown to be independent of ω for $\omega \ll \omega_J$, and ω/ω_J was chosen to be between $\frac{1}{30}$ and $\frac{1}{10}$. The value of k_m, typically 16 to 25, was chosen so that $k_m\omega_J \gg \omega_{LC}$; the value of k_m was varied to show that the values of $Z(\omega)$ did not depend on it.

The method was used to compute the spectral density of junction 4 shown in Fig. 11, and the corresponding values of $|Z_k|^2$ in Fig. 12. The complexity of the method does not easily allow the value of R to be voltage dependent, and the noise in Fig. 11 was computed with $R = 0.092\ \Omega$ for all voltages. This approximation gave rise to the discrepancy between the measured and predicted noise at low voltages in Fig. 11.

*Present address: Department of Physics and Materials Research Laboratory, University of Illinois at Urbana-Champaign, Urbana, IL 61801.

[1]W. C. Stewart, Appl. Phys. Lett. 12, 277 (1968).
[2]D. E. McCumber, J. Appl. Phys. 39, 3113 (1968).
[3]B. D. Josephson, Phys. Lett. 1, 251 (1962).
[4]V. Ambegoakar and B. I. Halperin, Phys. Rev. Lett. 22, 1364 (1969).
[5]A. N. Vystavkin, V. N. Gubankov, L. S. Kuzmin, K. K. Likharev, V. V. Migulin, and V. K. Semenov, Phys. Rev. Appl. 9, 79 (1974).
[6]H. Kurkijärvi and V. Ambegoakar, Phys. Lett. 31A, 314 (1970).
[7]R. F. Voss, J. Low Temp. Phys. 42, 151 (1981).
[8]K. K. Likharev and V. K. Semenov, Zh. Eksp. Teor. Fiz. Pis'ma Red. 15, 625 (1972) [JETP Lett. 15, 442 (1972)].
[9]R. H. Koch and J. Clarke (unpublished).
[10]C. M. Falco, W. H. Parker, S. E. Trullinger, and P. K. Hansma, Phys. Rev. B 10, 1865 (1974).
[11]R. J. Soulen, Jr. and R. P. Giffard, Appl. Phys. Lett. 32, 770 (1978).
[12]M. J. Stephen, Phys. Rev. 182, 531 (1969).
[13]A. J. Dahm, A. Denenstein, D. N. Langenberg, W. H. Parker, D. Rogovin, and D. J. Scalapino, Phys. Rev. Lett. 22, 1416 (1969).
[14]R. H. Koch, D. J. Van Harlingen, and J. Clarke, Phys. Rev. Lett. 45, 2132 (1980).

[15]H. B. Callen and T. A. Welton, Phys. Rev. 83, 34 (1951).

[16]Yu. M. Ivanchenko and L. A. Zil'berman, Zh. Eksp. Teor. Fiz. 55, 2395 (1968) [Sov. Phys.—JETP 28, 272 (1969)].

[17]A. J. Leggett, J. Phys. (Paris) C6, 1264 (1978).

[18]J. Kurkijärvi, in *Superconducting Quantum Interference Devices and their Applications,* edited by H. D. Hahlbohm and H. Lübbig (de Gruyter, Berlin, 1980), p. 247.

[19]A. O. Caldeira and A. J. Leggett, Phys. Rev. Lett. 46, 211 (1981).

[20]J. H. Greiner, C. J. Kircher, S. P. Klepner, S. K. Lahiri, A. J. Warnecke, S. Basavaiah, E. T. Yen, John M. Baker, P. R. Brosious, H.-C. W. Huang, M. Murakami, and I. Ames, IBM J. Res. Dev. 24, 195 (1980).

[21]J. Clarke and G. Hawkins, Phys. Rev. B 14, 2826 (1976).

[22]J. H. Claassen and P. L. Richards, J. Appl. Phys. 49, 4117 (1978).

[23]Y. Taur, IEEE Trans. Electron Devices ED-27, 1921 (1980).

[24]J. H. Claassen, Y. Taur, and P. L. Richards, Appl. Phys. Lett. 25, 759 (1974).

[25]R. P. Giffard, P. F. Michelson, and R. J. Soulen, IEEE Trans. Magn. MAG-15, 276 (1979).

[26]R. H. Koch, D. J. Van Harlingen, and J. Clarke, Appl. Phys. Lett. 38, 380 (1981).